Eur. Phys. J. B **14**, 543–549 (2000)

THE EUROPEAN PHYSICAL JOURNAL B

EDP Sciences

Ageing of random porous media following fluid deterministic displacement, freezing, thawing

Ju-Ping Tian[1,2,a] and Kai-Lun Yao[3,4]

[1] Physics Department of Wuhan Institute of Science and Technology, Wuhan 430073, P.R. China
[2] Physics Department of Huazhong University of Science and Technology, Wuhan 430074, P.R. China
[3] CCAST (World Laboratory), P.O. Box 8730, Beijing 100080, P.R. China
[4] International Center for Material Physics, Chinese Academy of Science, Shenyang 110015, P.R. China

Received 30 March 1999 and Received in final form 8 August 1999

Abstract. This paper introduces and investigates a simple model of random porous media degradation *via* several fluid displacing, freezing, and thawing cycles. The fluid transport is based on the deterministic method. The result shows that the topology and the geometry of porous media have a strong effect on displacement processes. The cluster size of the viscous fingering (VF) pattern in the percolation cluster increases with the increase of iteration parameter n. When iteration parameter $n \geq 10$, the VF pattern does not change with n. When $r \to 1$ and $n \geq 5$, the peak value of the distribution $N_{\rm mat}(r)$ increases as n increases; $N_{\rm mat}(r)$ is the normalized distribution of throat sizes after different displacement-damage but before the freezing. The distribution of throat size $N(r)$ after displacement but before freezing damage, shows that the major change, after successive cycles, happens at $r > 0.9$. The peak value of the distribution $N_{\rm inv}(r)$ reaches a maximum when $n \geq 10$ and $r = 1$, where $N_{\rm inv}(r)$ is the normalized distribution of the size of invaded throats for different iterations. This result is different from invasion percolation. The distribution of velocities normal to the interface of VF in the percolation cluster is also studied. When $n \geq 10$, the scaling function distribution is very sharp. The sweep efficiency E increases along with the increasing of iteration parameter n and decreases with the network size L. And E has a minimum as L increases to the maximum size of the lattice. The VF pattern in the percolation cluster has one frozen zone and one active zone.

PACS. 47.55.Mh Flows through porous media – 68.70.+w Whiskers and dendrites (growth, structure, and nonelectronic properties)

1 Introduction

The flow of fluids through random porous media plays an important role in a wide variety of environmental and technological processes. Examples include the spread of hazardous waste in soil, the displacement of oil in petroleum engineering, and some separation processes such as chromatography and catalysis. The displacement of a viscous oil by a less viscous solvent is inherently unstable. Even when the porous medium is homogeneous, viscous fingering (VF) will form, and reduce sweep efficiency. There are several experimental and theoretical methods to characterize the phenomenon. The first theoretical analysis by Saffmann and Taylor [1] was of the related problem of Hele-Shaw [2] flow. However, there are many differences between Hele-Shaw and porous media flow. In particular, reservoir rocks are rarely homogeneous. The porous media flow occurs in a discrete and highly chaotic network of pores and pore throats. Real porous media have a wide range of porosity, or of the concentration of open pores (occupying probability). As this concentration P decreases and approaches the percolation threshold $P_{\rm c}$, there appears a correlation length $\xi \sim |P - P_{\rm c}|^{-\nu}$ so the percolation network of open pores has a fractal geometry on length scales $L < \xi$. In many cases, physical phenomena exhibit a sharp crossover from a fractal behavior ($L < \xi$) to that of a homogeneous random system ($L > \xi$). Chen and Wilkinson [3] demonstrate that VF has the behavior for the $L > \xi$ case as they do in the uniform ($P = 1$) Hele-Shaw cell. Murat and Aharony [4] show that VF and DLA exhibit many different features in the vicinity of the percolation threshold.

Moreover, several studies [5] have shown that the freezing of water in porous media induces usually irreversible damage like fractures. The internal pore structure is strongly affected by the dilatation of the invading fluid under freezing. A well established statement is that the smaller a pore shape, the more damaged it will usually

[a] e-mail: jptian@jpi.cnpc.com.cn

become after freezing [6]. Recently, Salmon and Ausloos *et al.* [7] have studied a simple model of the fluid invasion-freezing-thawing cycle in porous media.

In the present study, the varying percolation clusters with varying occupation probabilities are first constructed. They correspond to connected porous media with the site as pore and the bond as throat; the radii of the throat follow the uniform distribution. Then, taking the center as the point of injecting, and aided by the successive over-relaxation technique, the VF pattern in the percolation clusters is obtained. Meanwhile, we will introduce and study a simple model of the fluid displacement-freezing-thawing cycles in porous media. From this, we study the ageing of the porous media after several displacement-freeze-thaw cycles under simple rules. The most simple one is illustrated below, and described in Section 2. It is assumed that the water density increases under freezing, and modifies (extends) the pore size. Other cases (see Sect. 2) have been examined without giving any other spectacular difference with respect to those given below. VF patterns in percolation cluster are shown (see Sect. 3). The kinetics of the invasion and the fractal dimension of VF pattern is investigated in Section 3. The velocity distribution is studied and discussed in Section 4 Sweep efficiency of displacement fluid is discussed in Section 4. Finally, Section 5 presents conclusions.

2 Model and simulation method

In a square lattice (201×201) with a given percolation probability P, while $P \geq 0.59$, a spanning cluster occurs; while $P = 1$ the occupying ratio of the site reaches 100%. The connectivity of the porous media varies according to the values of P. Those sites and clusters beyond the spanning cluster correspond to the non-connection areas of the sedimentary rocks. Our simulation is only concerned with the spanning cluster. The models of porous media and two-phase flow that we construct are as follows: The percolation clusters with varying occupation probability P correspond to varying porous media, with the site (node) as pore, the bond as throat, and the throat radius is normalized: $r \to (r - r_{\min})/(r_{\max} - r_{\min})$, where $r_{\min}$ and $r_{\max}$ are the minimum and maximum values of the throat radius. A similar model has also been used by some authors [7,23–25]. Therefore, a random number r_i between 0 and 1 is assigned to each throat i. The initial configuration of a 5×5 lattice is represented in Figure 1a. The center of the lattice is then injected with the invasion fluid. The displacement rule is as follows. At each time step, only a throat with the injected and displaced fluid is filled according to successive over-relaxation (see blow). The first displacement resulting from the 5×5 lattice of Figure 1a is drawn in Figure 1b. After the displacement fluid reaches the boundary of the percolation cluster, the fluid is assumed to freeze. In order to simulate some damage due to freezing, the size of each injected throat is assumed to increase according to the following rule [7]: $r_i \to r_i + \in (1 - r_i)$, where $\in$ is a random number taken from a flat distribution between 0 and 1. In so doing, $r_i(t+1)$ is always in $[r_i(t), 1]$. In some sense, this presupposes that the throat size itself follows the variation of the injected fluid density under freezing. An example of a damaged porous medium after the displacement in correspondence with that of Figure 1b is drawn in Figure 1c. The throat radius of the frozen fluid is then assumed to follow the formula $r_i \to r_i + \in (1 - r_i)$, and the medium to be completely dried up. A new fluid displacement can then take place. According to the normalized assumption of r, the maximum value of $r_i(t)$ is 1, no matter how $r_{\max}$ is increased. For example, if some the throat radius is $r_{\max}$, then $r_{\max}$ increases to $r_{\max} + \varepsilon (\varepsilon > 0)$ after freezing damage. Then, we have: $r \to [(r_{\max} + \varepsilon) - r_{\min})]/[(r_{\max} + \varepsilon) - r_{\min})$. Hence, it is inevitable that upon freezing the largest bonds ($r = 1$) never modify. We have investigated a 201×201 percolation lattice with P varying from 0.6 to 1, and iterations up to $n = 20$ have been simulated. It can be illustrated that our model is different from reference [7]. The model of Salmon and Ausloos *et al.* [7] is a pore freezing process, and our model is a throat freezing process. Moreover, the present invasion rule is also different from reference [7] which uses an invasion percolation rule in correspondence with the capillary forces control of fluid invasion. We use the deterministic method called successive over-relaxation technique [19] (see Fig. 1).

The simulation method used here has already been described in detail [10]. It is similar to the simulation by Chen and Wilkinson [3], with an extension to a finite viscosity ratio. The displacement is assumed to be piston-like down each tube. The flow rate (Q_{ij}) down the tubes connecting i and j is given by Poiseuille's law

$$Q_{ij} = \frac{\pi r_{ij}^4 (p_i - p_j)}{8[\eta_1 x_{ij} + \eta_2 (L - x_{ij})]} = g_{ij} \Delta p_{ij} \tag{1}$$

where p_i and p_j are the pressures at the ith and the jth node, respectively, η_1 and η_2 are the viscosity of the injected and displaced fluid, respectively, and $M = \eta_2/\eta_1$ (in this paper, $M = 10$) is the viscosity ratio and r_{ij} is the radius of bond ij, and x_{ij} is the length of bond ij occupied by the injected fluid. The quantity g_{ij} is the flow conductance of bond ij and is a function of time as the interfaces move. At each node we have the conservation equation

$$\sum_j Q_{ij} = 0. \tag{2}$$

We solve equations (2, 3) for the pressure field by successive over-relaxation iterations

$$p_i = \omega \frac{\sum_j g_{ij} p_j}{\sum_j g_{ij}} + (1 - \omega) p_i \tag{3}$$

where relaxation parameter ω is set to 1.66. The boundary conditions are such that at the point of injection

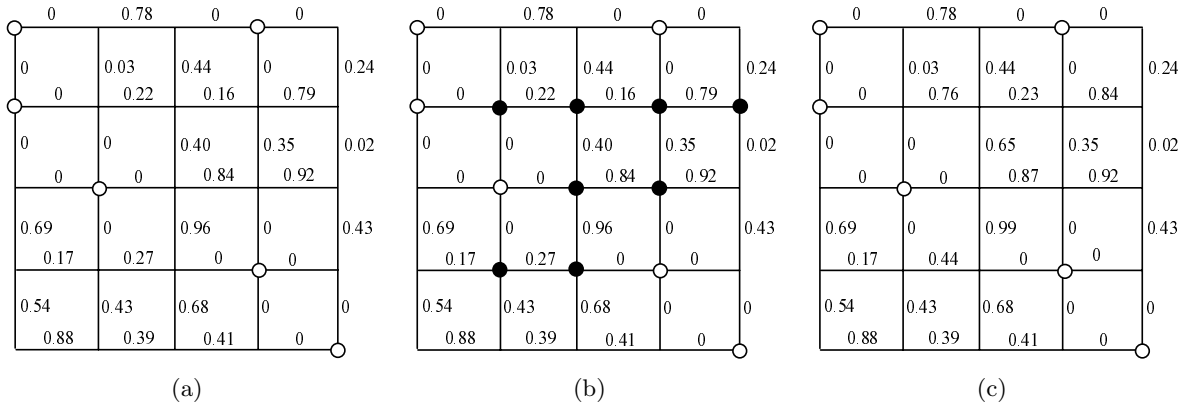

(a) (b) (c)

Fig. 1. Illustration of the displacement-freezing process. (a) A 5×5 lattice representing the porous medium. The lattice is a percolation cluster. The bond radii connected with a site (symbol: O) which is not occupied are all 0. (b) The displacement of the porous medium by a fluid (these sites are represented in dark). (c) The porous medium structure after the freezing process.

(center) $p = 1$, while at the point of production $p = 0$. After determining the nodal pressures we move the front a distance

$$\Delta x_{ij} = \frac{Q_{ij}}{\pi r_{ij}^2} \Delta t \tag{4}$$

into one of the pores adjacent to the interface. We choose the time step Δt to be the time necessary to exactly move the front to reach a node through the fastest tube. We then update all other fronts and for the new configurations of the regions of the displacing and displaced fluid, calculate the pressure field and repeat the entire process until the outer boundary is reached. This method has been used by many authors [3,8–23] to investigate VF. The main advantage of this method is that it allows us to investigate displacement process. It is also called the deterministic model [19]. While $n > 1$, in order to ensure the fluid conservation, when the displacement fluid enters the throat ij, it first occupies the room in the throat which comes from the enlarging of the radius, then goes on according to equation (5).

3 Evolution of the porous medium

Figure 2 shows the VF pattern in a percolation cluster ($P = 0.8$ and $M = 10$) for each of the first five iterations ($n = 1$, 2, 5, 10, 20). For $n = 1$, the VF pattern is a situation which has been studied [26]. For $n > 1$, the cluster size decreases with the increase of the iteration parameter n. It is obvious that the VF pattern shows almost no change when $n \geq 10$. The result is different from the invasion percolation [7]. Moreover, no mater what n is, the VF pattern grown in the percolation cluster has an anisotropy character. This result means that the geometry and the topology of the porous medium strongly affect the displacement processes and the structure.

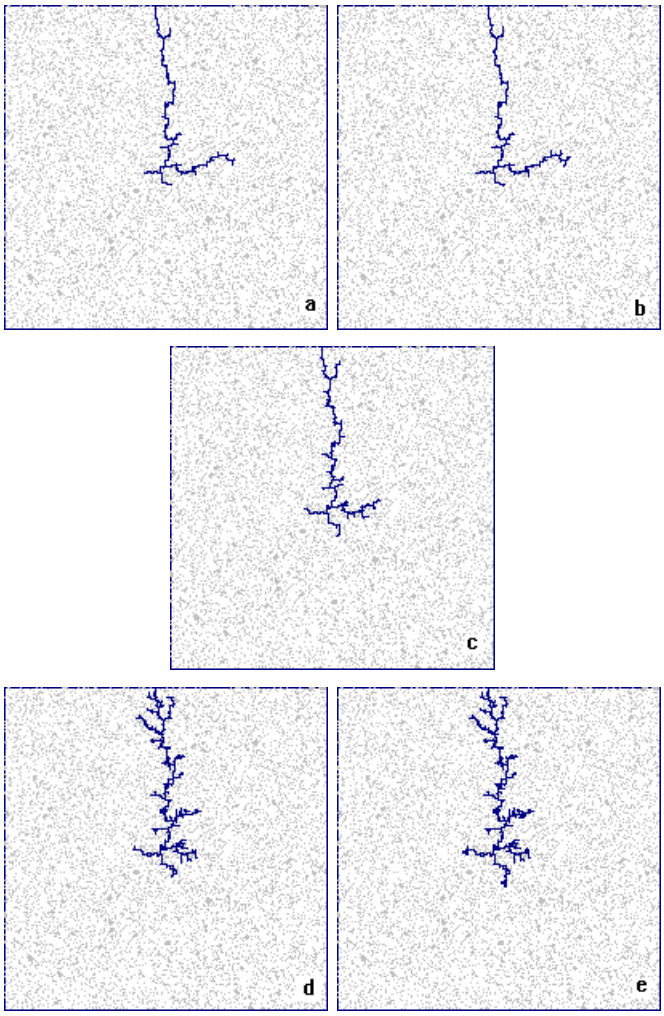

Fig. 2. Successive VF pattern with $P = 0.8$ in percolation cluster (a 201×201 lattice) after $n = 1$, 2, 5, 10 and 20 iteration, where, $n = 1$, 2, 5, 10 and 20 in correspondence with Figures 2a–2e.

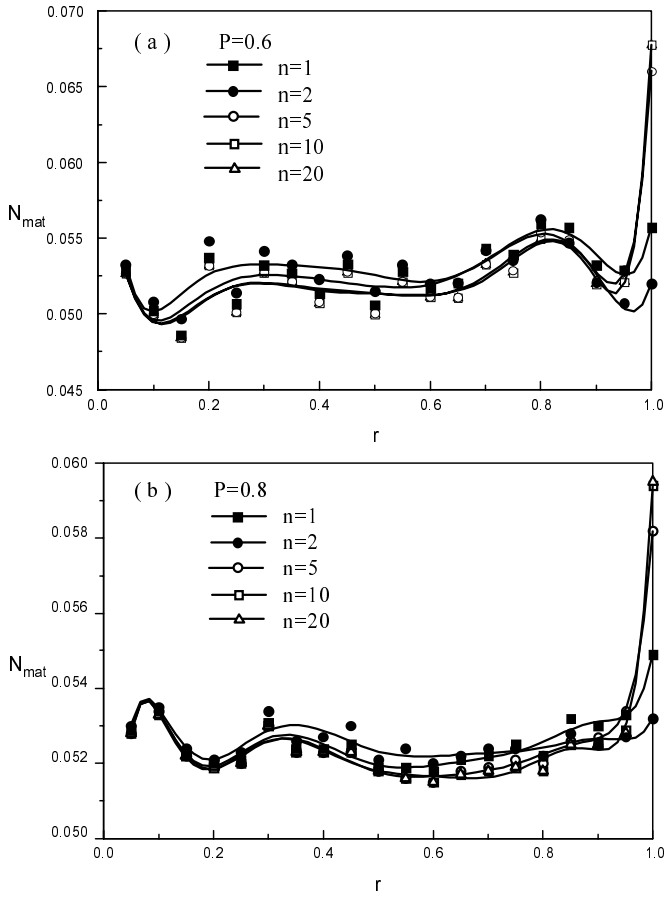

Fig. 3. The normalized distribution of throat sizes $N_{\rm mat}(r)$ in the percolation cluster is different displacement damages: $n = 1$, 2, 5, 10 and 20. (a): $P = 0.6$, (b): $P = 0.8$.

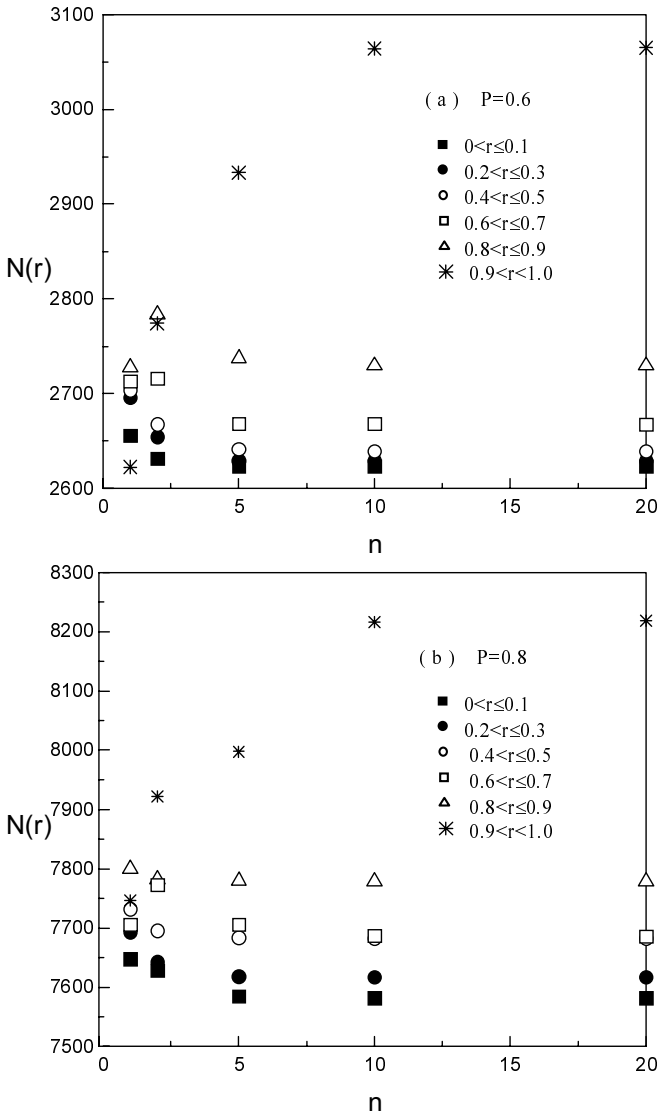

Fig. 4. A plot of $N(r)$ *vs.* n.

In Figure 3, the normalized distribution of throat size after the displacement but before freezing, $N_{\rm mat}(r)$, shows that the major change after successive cycles happens at $r = 1$. With increasing n, a peak occurs at $r = 1$ whereas the distribution below $r < 0.9$ is relatively flat and slightly decreases, as expected, with n. This suggests that the deterministic model selectively chooses a larger throat size for displacement (the reason will be explained a little later). This is also supported by the observation that $N_{\rm mat}(r = 0.05)$ does not change at all with n.

A plot of $N(r)$ *vs.* n is shown in Figure 4, where $N(r)$ is the distribution of throat sizes after displacement but before freezing damage. The major change, after successive cycles, happens at $r > 0.9$. And when $r > 0.9$, $N(r)$ is the same for $n = 10$ and $n = 20$. This means that the structure of VF is stable for the above mentioned condition. As seen in Figure 4, the transition to a more stable structure definitely happens between $n = 1$ and $n = 5$.

Figure 5 presents the normalized distribution of sizes of invaded throats, $N_{\rm inv}(r)$, for different iterations $n = 1$, 2, 5, 10 and 20. The peak value of the distribution $N_{\rm inv}(r)$ reaches a maximum when $n \geq 10$ and $r = 1$. That means the distribution $N_{\rm inv}(r)$ becomes stable when $n \geq 10$. For the invasion percolation [7], when $n = 1$, $N_{\rm inv}$ is zero almost for $r \geq 0.6$, which is different from our result (see Fig. 5). This also suggests that the deterministic model selectively chooses larger throat sizes for displacement. But it is just the opposite for the invasion percolation model [7]. The reason can be explained as follows: The invasion percolation model is consistent with that at low capillary number, water is injected slowly into a porous medium filled with oil, the capillary force dominates the viscous forces, and the dynamics is determined by the local pore radius r. Capillary forces are the strongest at the narrowest pore necks. Hence, the viscous forces are negligible in both fluids, and the principal force is due to capillary action. At every time step the invading fluid is advanced to the growth site that has the lowest random number r. But, our model is a deterministic growth model. In the viscous fingering, the principal force is due to the viscosity of the displaced; the viscous forces dominate the capillary force and the capillary effect is negligible. At every time step Δt (see Eq. (5)), the displacing fluids reach a node

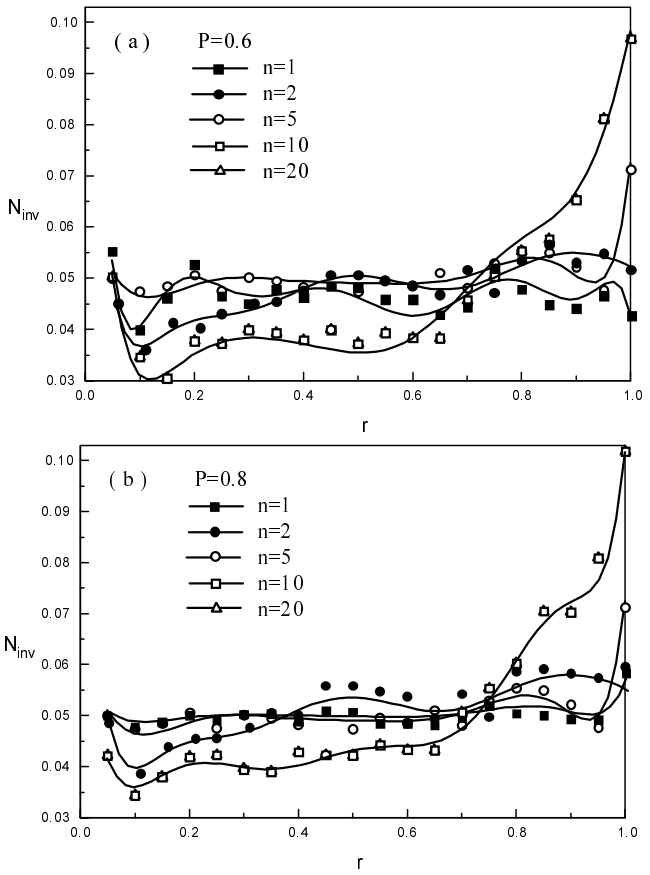

Fig. 5. The sizes distribution $N_{\rm inv}(r)$ of invaded throat in the percolation cluster after different iterations $n = 1$, 2, 5, 10 and 20. (a): $P = 0.6$, (b): $P = 0.8$.

(site) through the fastest tube according to equation (5) rather than the lowest random number r. Moreover, according to equation (2), the flow conductance g_{ij} is equal to $\pi r_{ij}^4/8[\eta_1 x_{ij} + \eta_2(L - x_{ij})]$. This means that $g_{ij} \propto r_{ij}^4$. Hence, the deterministic model chooses larger throat sizes for displacement.

To show the influence of topology and geometry of the porous medium on the structure of VF, we obtained the pattern of VF with $M = 10$ for different probability P at different parameter n. The fractal dimensions D are calculated at different probabilities P at different iterations n. In order to estimate D, we have measured the cluster size S of VF's pattern for different lattice size $L \times L$ and for different iteration n and occupation probability P. Assuming the relationship [7]: $S \sim L^D$, in Figure 6, we can see that the fractal dimension D of VF is the same. When $P = 1$, no matter what n is, $D = 2$. This means the structure of the VF cluster is compact at a finite viscosity ratio M in the two dimensional square lattice. No matter what P is, the fractal dimension D of VF is the same for $n = 10$ and $n = 20$. This means that the structure of VF is stable for $n \geq 10$. Moreover, no matter what n is, the fractal dimension D increases along with the increase of occupation probability P. This shows that the topology and geometry of the porous medium strongly affect on the displacement process.

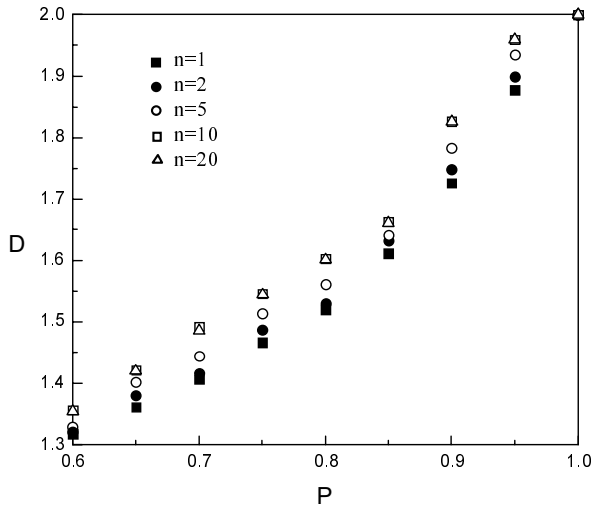

Fig. 6. The fractal dimension D as function of occupation probability P.

4 The velocity distribution and sweep efficiency

In this paper, we also study the distribution of velocities normal to the interface in the percolation cluster. The method is described in detail in reference [20]. After each group of sites has been added, all the interfacial velocities are analyzed, the root-mean square cluster radius R is measured, and the total number of filled sites and surface sites is recorded. Surface sites are nodes filled with the displacing fluid, but with one or more nearest neighbours occupied by the displaced fluid. At each stage, we make a histogram of the velocity distribution, sorting the velocities into equally spaced logarithmic bins. The number N in each bin, assuming the scaling hypothesis, will be given by

$$N\mathrm{d}[\ln(V)] = R^{f(\alpha)}\mathrm{d}(-\alpha) \tag{5}$$

where the velocity V is equal to $R^{-\alpha}$ and $\mathrm{d}[\ln(V)]$ is the width of the logarithmic bin. Hence, $\alpha = -\ln(V)/\ln(R)$ and $\mathrm{d}[\ln(V)] = \mathrm{d}(-\alpha)\ln(R)$. This gives us a scaling function

$$f(\alpha) = \frac{\ln[N\ln(R)]}{\ln(R)}\,. \tag{6}$$

Figure 7 shows the effect of randomness on the velocity distribution at viscosity ratios $M = 10$ and $P = 0.8$. The tail of the distribution (large α) is longer for the small parameter n. When $n \geq 10$, the distribution is very sharp. And when $n = 10$, 20, $f(\alpha)$ curve is fully a coincidence. That means the velocity distribution $f(\alpha)$ becomes stable when $n \geq 10$.

A particularly useful area is in the prediction of sweep efficiencies E [19] ($= A_{\rm e}/A_{\rm s}$), where, $A_{\rm e}$ and $A_{\rm s}$ are respectively the sweep area and the percolation cluster's area in sweep region, respectively. Figure 8 shows that the sweep

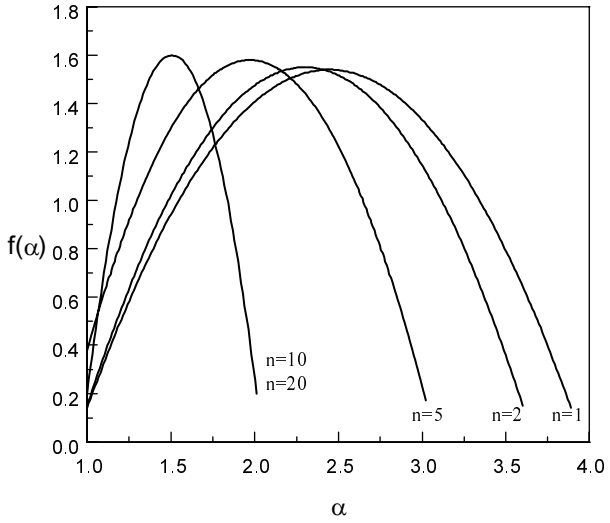

Fig. 7. Scaling function $f(\alpha)$ and the effect of the iteration parameter $P = 0.8$.

efficiency E decreases along with the increasing of the iteration parameter n and the network size L. It is apparent that E has a minimum as L increases to the maximum. It is interesting to note that the $E \sim L$ curve has two linear regions. That means the VF pattern has a frozen zone and an active zone [27].

5 Conclusions

In this paper, we have introduced and investigated a simple model of porous media degradation *via* several fluid displacing, freezing, and thawing cycles. The fluid transport is based on a deterministic model. The development of the model toward a more realistic one with other constraints is obvious. And our model is different from reference [7]. The model of Salmon and Ausloos *et al.* [7] is for a pore's freezing process, and our model is a throat's freezing process. Moreover, the invasion rule is also different from reference [7] which uses the invasion percolation rule in which the capillary forces control the fluid invasion. The successive over-relaxation technique (the deterministic method) [19] is used in this paper. The distribution of throat size $N(r)$ after displacement but before freezing damage, shows that the major change, after successive cycles, happens at $r > 0.9$. And when $r > 0.9$, $N(r)$ is the same for $n = 10$ and $n = 20$.

The cluster size of the VF pattern in the percolation cluster increases with the increase of iteration parameter n. When $n \geq 10$, the VF pattern almost does not change. The peak value of the distribution $N_{\rm inv}(r)$ reaches a maximum when $n \geq 10$ and $r = 1$. This result is different from invasion percolation [7]. No matter what n is, the fractal dimension D increases along with the increase of the occupation probability P. This shows that the topology and geometry of the porous medium have a strong effect on the displacement process.

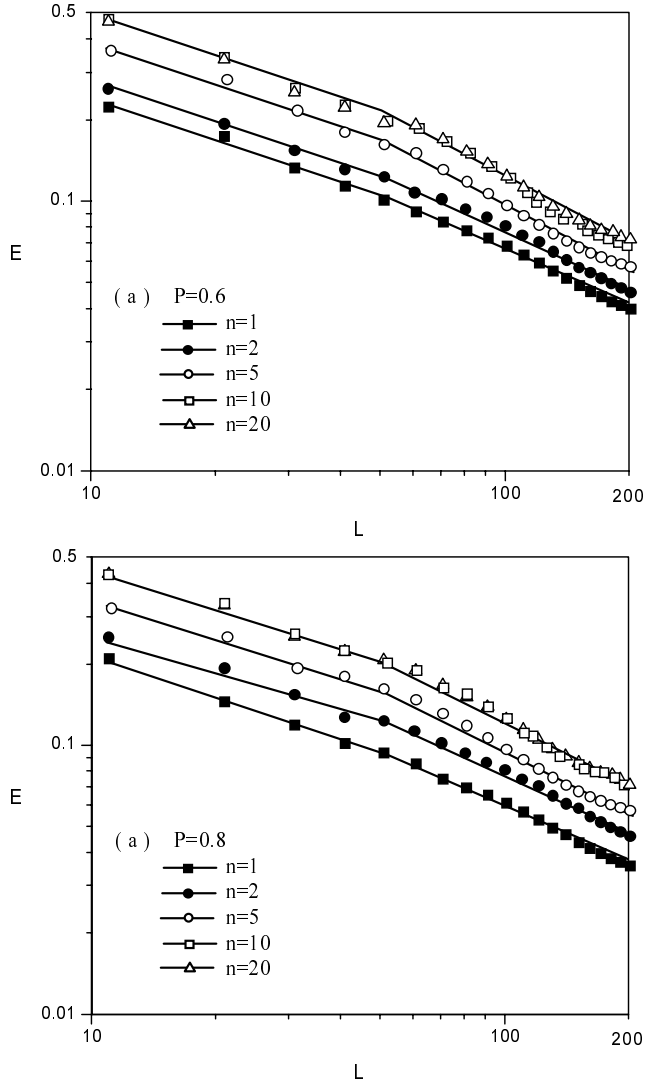

Fig. 8. Sweep efficiency E as a function of network size L, when $M = 10$. (a) $P = 0.6$, (b): $P = 0.8$.

The tail of the scaling function distribution $f(\alpha)$ (large α) is larger for the smaller parameter n. When $n \geq 10$, the scaling function distribution is very sharp. The sweep efficiency E increases along with the increasing of the iteration parameter n and decreases along with the increasing of the network size L. E reaches a minimum as L increases to the maximum size of the lattice. The VF pattern in the percolation cluster has a frozen zone and an active zone.

The author would like to thank Prof. M. Ausloos for his useful help. We have refered to a computer program which is provided generously by Prof. Ausloos. This work is supported by the National Natural Science Foundation of China (No. 19774023) and by the National High Performance Computing Foundation of China (No. 984050).

References

1. P.G. Saffman, G.I. Taylor, Proc. R. Soc. A **245**, 312 (1958).
2. H.S. Hele-Show, Nature **58**, 34 (1898).
3. J.D. Chen, D. Wilkinson, Phys. Rev. Lett. **55**, 18 (1985).
4. M. Murat, A. Aharony, Phys. Rev. Lett. **57**, 1875 (1986).
5. M. Nakamura, T. Fukushima, M. Kamitani, J. Ceram. Soc. Jpn **100**, 853 (1992).
6. N. Lens, R. Gerard, F. de Barquin, J. Elsen, CSTC Mag. **3**, 12 (1996).
7. E. Salmon, M. Ausloos, N. Vandewalle, Phys. Rev. E **55**, R6348 (1997).
8. M. Sahimi, Y.C. Yortsos, Phys. Rev. A **32**, 3762 (1985).
9. M.J. King, H. Scher, Phys. Rev. A **35**, 929 (1987).
10. U. Oxaal, Phys. Rev. A **44**, 5038 (1991).
11. U. Oxaal, F. Boger, J. Feder, T. Jøssang, P. Meakin, A. Aharony, Phys. Rev. A **44**, 6564 (1991).
12. M.J. Blunt, M.J. King, H. Scher, Phys. Rev. A **46**, 7680 (1992).
13. M.J. Blunt, H. Scher, Phys. Rev. E **52**, 6387 (1995).
14. P. Meakin, G. Wagner, J. Feder, T. Jøssang, Physica A **200**, 241 (1993).
15. P. Meakin, J. Feder, V. Frette, T. Jøssang, Phy. Rev. A **46**, 3357 (1992).
16. V. Frette , J. Feder, T. J_ssang, P. Meakin, Phy. Rev. Lett. **68**, 3164 (1992).
17. J.D. Chen, D. Wilkinso, Phys. Rev. Lett. **55**, 18 (1985).
18. P.R. King, J. Phys. A **20**, L529 (1987).
19. H. Siddiqui, M. Sahimi, Chem. Eng. Sci. **45**, 163 (1990).
20. M.J. Blunt, P.R. King, Phys. Rev. A **37**, 3935 (1988).
21. R. Lenormand, E. Touboul, C. Zarcone, J. Fluid Mech. **189**, 165 (1988).
22. M. Ferer, R.A. Geisbrecht, W.N. Sams, D.H. Smith, Phys. Rev. A **45**, R6973 (1992).
23. J.P. Tian, K.L. Yao, ACTA Phys. Sinica **7**, 681 (1998).
24. R.W. Flumerfelt, H.L. Chen, Wirogana Ruengphrathuengsuka, W.F. Hsu, J. Prieditis, SPE Formation Evaluation **7**, 25 (1992).
25. J.P. Tian, K.L. Yao, Chin. Phys. Lett. **15**, 577 (1998).
26. J.P. Tian, K.L. Yao, Phys. Lett. A **251**, 259 (1999).
27. H. Boularot, G. Albinet, Phys. Rev. E **53**, 5106 (1996).